

Role of Al, Ti, and Zr in Gray Iron Preconditioning/Inoculation

Iulian Riposan, Mihai Chisamera, Stelian Stan, Chris Ecob, and David Wilkinson

(Submitted June 20, 2007; in revised form January 21, 2008)

A research was done to investigate the effect of strong deoxidizing elements, such as Al, Zr, and Ti, in gray irons in laboratory experiments. The conclusions drawn were based mainly on thermal analysis, chill (carbides) sensitivity, graphite characteristics, and SEM analysis. Al and Zr have visible beneficial effects in preconditioning of gray irons, by favoring lower undercooling during solidification. Ti has an inconclusive role, with limited influence, but promotes undercooled graphite formation. Complex (Mn,X)S compounds, nucleated on the previously formed small oxide-based sites, were found as the major nucleation sites for graphite in gray irons, with specific distribution of Al, Ti, and Zr. Al,Zr-FeSi preconditioning of electrically melted and Sr-FeSi inoculated gray irons avoided type D graphite and carbides in 3 mm sections castings.

Keywords Al, Ti, Zr, graphite nucleants, graphitizing, gray iron, preconditioning

1. Introduction

As is generally accepted, the inoculation effect on graphite nucleation in gray irons is based upon the formation of complex non-metallic microinclusions (sulfides, oxides, silicates, nitrides, and carbides) having a sufficient crystallographic symmetry to essentially match that of graphite. In this respect, the inoculants chemistry usually includes active elements which have high affinity especially toward oxygen, sulfur, and nitrogen, such as Ca, Ba, Sr, Al, Ti, Zr, RE, etc.

A larger number of microinclusions that may act as possible nucleation sites for graphite in un-inoculated and inoculated gray irons have been examined using different electron microscopy techniques (Ref 1-6). Based on these analyses, the following three-stage model for graphite nucleation was proposed: Stage (1): Microinclusions based on strong deoxidizing elements, such as Mn, Si, Al, Ti, and Zr are formed in the melt. Stage (2): Nucleation of (Mn,X)S compounds on these microinclusions in the melt. In un-inoculated irons X = Fe (mainly) and to a lesser extent X = Ca, Al, or Ti. In addition, the Mn level and Mn/S ratio in the compounds are higher. In inoculated irons X = Ca, Sr, Ba, Al, RE, etc., in addition the Mn level and Mn/S ratio in the compound is lower. A thin layer of silicate may form at the surface of the (Mn,X)S compound in the inoculated iron. Stage (3): Graphite nucleates on the (Mn,X)S compound. In un-inoculated iron the (Mn,X)S compound is simple and the crystallographic mismatch

between the graphite and the compound is relatively large. In inoculated iron, the (Mn,X)S compound is more complex and the crystallographic mismatch between the graphite and the compound is lower.

It was found that Al contributes to the formation of AlO-based sites which act as nucleation sites for (Mn,X)S compounds (Fig. 1) even at a very low level (<0.003 wt.% Al) in the iron melt. Increasing the residual Al content in iron melt helps the initiation of graphite nucleation with a lower degree of undercooling. A 0.005-0.010 wt.% Al content in the melt appears to be beneficial, without the detrimental effect of pinhole occurrence in gray cast irons (Ref 4-6).

The main objective of the present investigation was to compare the strong deoxidizing elements, such as aluminum, zirconium, and titanium, to determine their individual capacity toward preconditioning of un-inoculated and Sr-inoculated gray cast irons.

2. Al, Zr, and Ti Comparison

2.1 Experimental Procedure

To ensure a low level of trace elements, a relatively pure charge was used in the experiment consisting of 90% synthetic pig iron (3.64% C, 1.69% Si, 0.34% Mn, 0.014% S, 0.02% P, 0.001% Al, 0.003% Ti) and 10% selected steel scrap (0.04% C, 0.01% Si, 0.17% Mn, 0.01% S, 0.01% P, 0.045% Al, 0.006% N). High purity FeSi (74.6% Si, 0.006% Al), FeMn80, FeP18, FeS₂, and graphite re-carburizer were used for the correction of chemical composition of the iron melt in the acid-lined induction furnace.

Experimental heats were superheated up to 1500 °C, with 10 min holding at this temperature before tapping. The iron melt was tapped at 1450 °C into small ladles (3 kg iron, acid lined). Three different preconditioning elements (Al, Ti, or Zr) were added, at the same level (0.03 wt.%) into the melt stream during tapping (Fig. 2). The melt was mechanically stirred in each ladle (steel rod). Al-metallic (99.5% Al), Ti-metallic (99.5% Ti), and FeSiZr (43.5% Si, 30.8% Zr, and 0.56% Al)

Iulian Riposan, Mihai Chisamera, and Stelian Stan, POLITEHNICA University of Bucharest, 313 Spl. Independentei, 060042 Bucharest, Romania; and Chris Ecob and David Wilkinson, ELKEM Foundry Products Division, P.O. Box 8040, Vaagsbygd, 4675 Kristiansand S, Norway. Contact e-mails: riposan@tmnc.foundry.pub.ro and chris.ecob@elkem.no

were used as preconditioning agents. A highly accurate analytical balance was used to evaluate each addition rate.

One series of experimental irons (a reference and with different preconditioning elements) were used in un-inoculation conditions. The second series of irons, with the same make-up, was inoculated in the ladle with low aluminum, Sr-FeSi alloy (76.9% Si, 0.8% Sr, 0.01% Al, <0.0005% Ti). Inoculant was added (0.3 wt.%) at 1400-1420 °C after deslagging on the melt surface and was mechanically stirred for about 1 min (steel rod).

Experimental un-inoculated and inoculated irons were poured into test castings made from furan no-bake bonded molds. The test castings all were poured at 1380-1400 °C. The specially designed test mold included a central down sprue which simultaneously supplied un-inoculated or inoculated iron to three separate test samples. A wedge test specimen and a forced chill test specimen, both of them 50 mm high and 75 mm long were used for chill tendency evaluation (Fig. 3). A round bar specimen (20 mm diameter, 100 mm high) was used for cooling curve recording (K-type thermocouple was incorporated) and structure characterization, respectively. After casting, the chill test samples and bars were allowed to cool to room temperature before they were shaken out.

2.2 Results and Discussion

2.2.1 Final Chemical Composition. The cast irons, both un-inoculated and inoculated, with different sources of preconditioners, showed reasonable consistent content of carbon (3.15-3.29% C), silicon (1.49-1.67% Si), manganese (0.55-0.63% Mn), sulfur (0.096-0.10% S) and phosphorus (0.20-0.21% P). Other residual elements were kept at negligible low

levels (Table 1). The aluminum content was 0.002-0.004% Al range in the normal irons and at 0.027-0.028% Al level in Al-treated irons. Similarly, the titanium content was varied from 0.003-0.005% Ti in normal irons, to 0.011-0.017% Ti in Ti-enriched irons. Zirconium was detected in the iron melt at 0.011-0.013% Zr level only in Zr-added irons, by direct coupled plasma (DCP) analysis technique.

2.2.2 Chilling Tendency. The specimen was struck with a hammer in such a manner that the fracture was straight and midway along the length. The design of the wedge test specimen and the contact of the forced chill test specimen with the metallic chill plate promoted accelerated cooling rates (higher for the second specimen type) and favor the formation of chill at the apex of specimens (Fig. 3). The chilled iron consists of two zones. The chill from the apex or the chilled face to the first appearance of a gray spot was designated as clear chill. The distance from the apex or the chilled face to the last appearance of a spot of white iron was designated as total chill. That portion of the chill affected zone between the clear chill and the total chill was designated as the mottled zone.

A comparison of the effectiveness of the Al, Ti, and Zr preconditioning on chill depth in un-inoculated and inoculated irons is shown in Table 2. The graphs in Fig. 4 summarize the test data of chill depth versus deoxidizers type (Al, Ti, and Zr) and cooling rate level (wedge or forced chill specimen), as clear chill and total chill evaluation. At low level of carbon (3.15-3.16% C), silicon (1.49-1.53% Si), and carbon equivalent (3.70-3.72% CE), un-inoculated irons are characterized by having high chilling tendency. Inoculation gave, as expected, overall lower chill than with no inoculation. Very low level of chilling tendency for inoculated irons illustrates the efficiency of this treatment for the optimum content of sulfur (0.096-0.10% S) and manganese to sulfur ratio (Mn/S = 5.6-6.5) conditions, respectively.

Preconditioning (Al, Ti, and Zr) of the iron during the tapping period appears to have a beneficial effect in both un-inoculated and inoculated irons, for both cooling rate levels and for both chilling properties evaluation. Importantly, for the same addition rate, in the same pouring technique and solidification parameters, different effects of Al, Ti, and Zr were found.

Titanium seems to be beneficial only in un-inoculated irons and clear chill evaluation, especially during lower cooling rate solidification (wedge test specimen). Zirconium and aluminum are more effective in all conditions, with zirconium having the

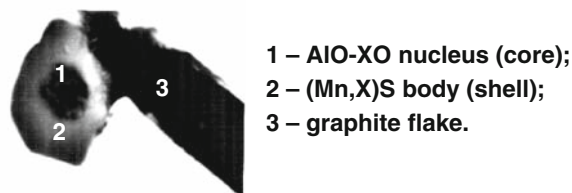


Fig. 1 Three-stage model for the nucleation of graphite in gray iron

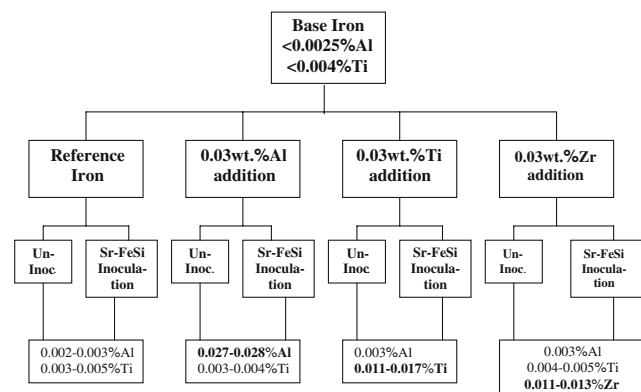


Fig. 2 General schedule of laboratory experiments and final Al, Ti, and Zr content

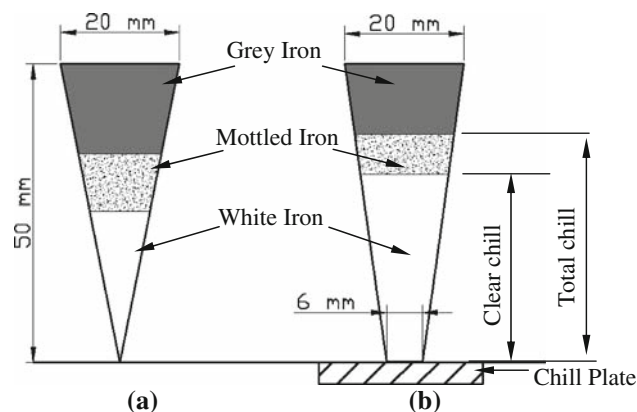


Fig. 3 Wedge test (a) and Forced Chile test (b) samples

Table 1 Chemical Composition of Final Cast Irons

Iron	Heat	0.03 wt.%	Chemical composition (a), wt.%								CE, %	Mn/S
			C	Si	Mn	S	P	Al	Ti	Zr		
Un-inoculated	1	...	3.15	1.49	0.62	0.10	0.20	0.002	0.003	0.011	3.70	6.2
	2	Al	3.15	1.53	0.63	0.098	0.20	0.028	0.003		3.71	6.4
	3	Ti	3.16	1.51	0.62	0.096	0.20	0.003	0.011		3.72	6.5
	4	Zr	3.15	1.52	0.62	0.097	0.20	0.003	0.004		3.71	6.4
0.3% Sr-FeSi	5	...	3.29	1.67	0.57	0.097	0.21	0.003	0.005	0.013	3.90	5.9
	6	Al	3.27	1.65	0.57	0.097	0.21	0.027	0.004		3.87	5.9
	7	Ti	3.22	1.64	0.55	0.096	0.21	0.003	0.017		3.82	5.7
	8	Zr	3.20	1.67	0.55	0.099	0.21	0.004	0.005		3.81	5.6

(a) Minor elements, (max): 0.06% Cu, 0.03% Ni, 0.05% Cr, 0.015% Mo, 0.003% V, 0.0018% Nb, 0.006% Sn, 0.001% Pb, 0.004% Sb, and 52-53 ppm N

Table 2 Chill, eutectic undercooling degree, and structure characteristics

Iron	Heat	0.03 wt. %	Depth of chill, mm				Under-cooling degree, ΔT_1 , °C	Graph, %	Under-cooled graphite, (D + E)%	Carbides, %
			Wedge test		Forced chill test					
			Clear	Total	Clear	Total				
Un-inoculated	1	...	22	50	28	50	-10.1	0-3	100	35
	2	Al	11	23	18	28	-5.3	3-6	60	15
	3	Ti	11	50	23	50	-8.1	0-5	90	30
	4	Zr	0	13	10	23	-6.4	8-10	65	5
0.3% Sr-FeSi	5	...	2	4	8	12	-0.9	8-12	5	0
	6	Al	0	0	4	7	+3.1	8-12	...	0
	7	Ti	0	3	7	13	+1.2	8-12	15	0
	8	Zr	0	0	0	8	+3.8	8-12	...	0

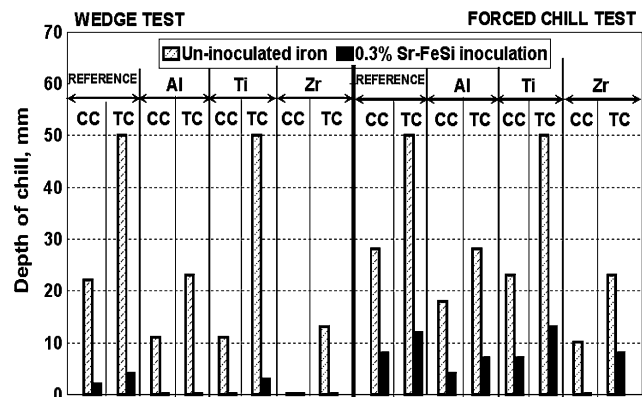


Fig. 4 Influence of Al, Ti, and Zr preconditioning on the chill parameters (CC—clear chill; TC—total chill)

higher efficiency. In wedge test solidification conditions, clear chill was avoided by the Zr addition, in un-inoculated irons, while total chill was at the same level as clear chill for Ti-addition, for both un-inoculated and inoculated irons.

The chilling properties of the experimental irons (Fig. 4) correlate well with the degree of the eutectic undercooling, especially at the beginning of eutectic solidification ($\Delta T_1 = TEU - T_{mst}$ parameter, Fig. 5). The lowest ΔT_1 level, the highest chill depth, in both un-inoculated and inoculated irons. The equilibrium eutectic temperature in the metastable/carbidic

system (T_{mst}) was calculated as the most influenced by silicon content ($T_{mst} = 1147 - 12\% Si$). The low eutectic temperature (TEU) was determined from cooling curve analysis. At negative values, the ΔT_1 parameter illustrates the white iron solidification pattern. In experimental conditions, all of un-inoculated irons start the eutectic reaction under the carbidic eutectic temperature ($\Delta T_1 < 0$), but at different levels depending on the preconditioning agent: Al and Zr are better than Ti. Inoculation moved the irons to positive value of this parameter, but also with Al and Zr being more effective.

2.2.3 Structure Characteristics. The effects of Al, Ti, and Zr were further examined comparing the microstructure of 20 mm diameter bars, specifically graphite amount (area), undercooled graphite (D + E-type), and the amount of free carbides (Table 2).

A mottled structure for un-inoculated irons and a gray structure for inoculated irons is the major characteristic of the experimental irons. Un-inoculated irons are more sensitive to active elements addition: the lowest graphite amount is typically for reference and Ti-added irons, an increased graphite amount in Al-added iron and the highest levels with a Zr addition.

Undercooled graphite morphologies (type D and E) and free carbides occurrence is typical for the un-inoculated irons (Fig. 6). Inoculation was efficient in avoiding carbides, while undercooled graphite is predominant in the reference iron and in the Ti-added iron. The ranking of active elements appears to be as before, especially in un-inoculated irons.

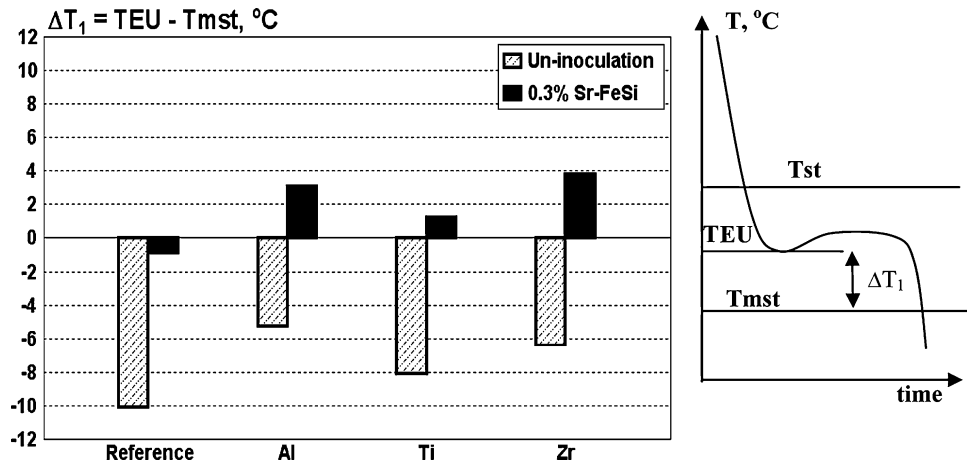


Fig. 5 Influence of Al, Ti, and Zr preconditioning on the ΔT_1 —eutectic undercooling parameter

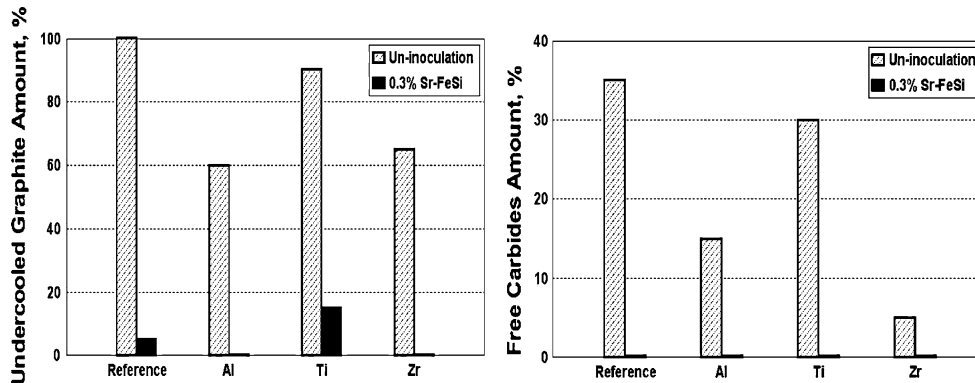


Fig. 6 Influence of Al, Ti, and Zr preconditioning on the undercooled graphite ($D + E$) (a) and free carbides (b) amount

2.2.4 SEM Analysis. SEM Analysis was performed by a Philips SEM-515 instrument equipped with EDS microanalyzer.

It was re-confirmed that complex $(Mn,X)S$ compounds act as nucleation sites for graphite flakes in gray of cast irons. Graphite begins growing on the surface irregularities of $(Mn,X)S$ compounds (edge, picks, and roughness). Complex compounds morphology gives a higher graphite branching tendency, while smaller size and higher compactness particles favor more simple and lower branching tendency of graphite.

Small particles, a quasi-regular polygonal shape, are typically for Al and Zr preconditioning (Zr-generates twice the number of particles as Al). Larger particles, with the lowest count and mainly indented outline (like a dendrite) characterizes Ti-preconditioning irons (Fig. 7). It was found that Al, Zr, and Ti have different distribution pattern, into the core (nucleus) and shell (body) of $(Mn,X)S$ compounds:

- Al was present in all compounds, both with and without Al addition, and including in Ti- or Zr-added irons, mainly located in the nucleus of these complex sulphides (the highest level in Al-preconditioned irons).
- Zr was found only in Zr-added irons, at high level in the nucleus, but also at important level in the shell of $(Mn,X)S$ compounds.
- Ti has a lower incidence in conventional irons, but with a significant presence in Ti-added irons, mainly located in the core, with peculiar presence in the shell at higher content.

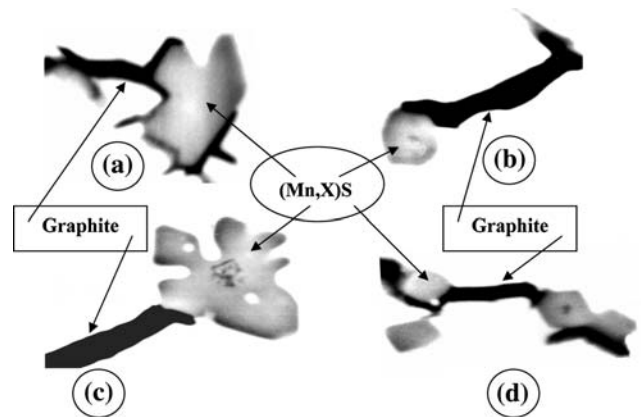


Fig. 7 Typical growing view of graphite on $(Mn,X)S$ particles as nucleation sites, in un-preconditioned (a), Al (b), Ti (c), and Zr (d) preconditioned irons [SEM, 5000:1]

3. Al, Zr-Fesi Alloy as Preconditioner

It was found that the both strong deoxidizers, Al and Zr, are able to promote higher compactness and small nucleation sites, with high-graphitization capacity, consequently graphite with lower branching grade (A-type) resulted. Based on this

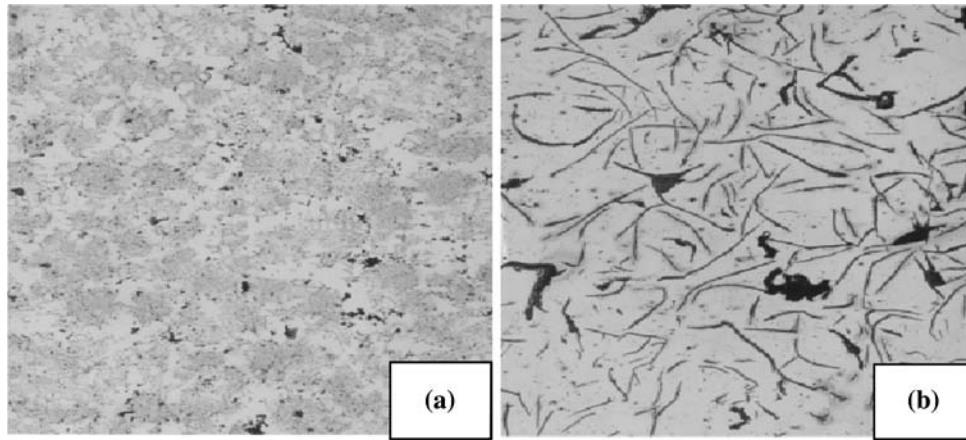


Fig. 8 Structure change as 0.1 wt.% Al,Zr-FeSi preconditioning of electrically melted gray cast iron: (a) without preconditioner and (b) preconditioned iron (100:1; 2% Nital etched)

research, a new complex preconditioner was designed and tested in laboratory experiments and plant trials, in a large diversity of conditions.

A foundry case study is represented to illustrate the efficiency of Al and Zr bearing-FeSi complex alloy preconditioning of electrically melted gray iron. The foundry is a gray iron domestic rainwater fittings producer with casting breakages in transit as the major problem. A coreless induction furnace was used. The metallic charge included 35% steel scrap, 35% cast iron scrap, and 30% foundry pig iron. Tapping was recorded at 1500 °C with the pouring at 1420-1450 °C. Ladle inoculation is the usually procedure with 0.25% Sr-FeSi inoculant addition rate. Typical structure changes are shown in Fig. 8. Without preconditioning, structure consists mainly of 80% types D and E graphite and dispersed carbides (Fig. 8a). Addition of 0.1% of Al,Zr-FeSi alloy to the melt furnace resulted in to 90% type A and 10% type B graphite, without undercooled graphite or free of carbides in 3 mm sections castings (Fig. 8b). Casting breakages were eliminated.

4. Conclusions

- Less than 0.005% Al and Ti electrically melted base iron was preconditioned up to 0.027-0.028% Al, 0.011-0.017% Ti or 0.011-0.013% Zr, with the same 0.03 wt.% addition of Al, Ti, or Zr.
- Al and Zr have visible beneficial effects, by lowering the degree of eutectic undercooling, chilling tendency, undercooled graphite, and free carbides amount, in both un-inoculated and inoculated irons.
- Ti seems to be beneficial as graphitizing action only in un-inoculated irons, but at lower relative power compared to Al and Zr.
- It was re-confirmed that complex (Mn,X)S compounds nucleated on the previously formed very small oxide based sites act as major nucleation sites for graphite flakes with specific distribution of Al, Ti, and Zr.

- Small particles with high number density and quasi-regular polygonal shape, favorable for type A graphite nucleation, are typically for Al and Zr preconditioning.
- Larger particles with the lowest numerical count and mainly indented outline (like a dendrite), are favorable for type D graphite formation, so characterizing Ti preconditioned irons.
- 0.1 wt.% Al,Zr-FeSi preconditioning of electrically melted gray iron in foundry conditions led to important structure changes, from mainly D and E type graphite and dispersed carbides to mainly A-type graphite without undercooled graphite or free carbides in 3 mm sections castings.

Acknowledgments

Laboratory research was conducted by POLITEHNICA University of Bucharest, Romania, with the collaboration and funds provided by ELKEM Foundry Products Division, Norway.

References

1. M. Chisamera, I. Riposan, S. Stan, and T. Skaland, Undercooling—Chill Size—Structure Relationship in the Ca/Sr Inoculated Grey Irons and under Sulphur/Oxygen Influence, *64th World Foundry Congress, Paris, France*, 2000, Paper RO-62
2. I. Riposan, M. Chisamera, S. Stan, T. Skaland, and M.I. Onsoien, Analyses of Possible Nucleation Sites in Ca/Sr Over-Inoculated Grey Irons, *AFS Trans.*, 2001, **19**, p 1151-1162
3. I. Riposan, M. Chisamera, S. Stan, and T. Skaland, Graphite Nucleant (Microinclusion) Characterization in Ca/Sr Inoculated Irons, *Intl. J. Cast Metal Res.*, 2003, **16**(1-3), p 105-111
4. I. Riposan, M. Chisamera, S. Stan, and T. Skaland, A New Approach to Graphite Nucleation Mechanism in Gray Irons, *Proceedings of the AFS Cast Iron Inoculation Conference, Sept. 29-30, 2005*, Schaumburg, USA, p 31-41
5. M. Chisamera, I. Riposan, S. Stan, and T. Skaland, Effects of Residual Aluminium on Solidification Characteristics of Un-inoculated and Ca/Sr Inoculated Grey Irons, *AFS Trans.*, 2004, **112**, p 867-877
6. I. Riposan, M. Chisamera, S. Stan, C. Gadarautanu, and T. Skaland, The Key Role of Residual Aluminium in Chill Tendency and Structure Characteristics of Un-inoculated and Ca/Sr Inoculated Gray Irons, *66th World Foundry Congress, Istanbul, Turkey*, 2004, p 775-789